THE JOURNAL OF PHYSICAL CHEMISTRY B

ARTICLE

pubs.acs.org/JPCB

Influence of Chain Length of Alcohols on Stokes' Shift Dynamics in Catanionic Vesicles

Namrata Sarma, Jayanta M. Borah, and Sekh Mahiuddin*

Materials Science Division, North-East Institute of Science and Technology, CSIR, Jorhat 785006, Assam, India

Harun Al Rasid Gazi, Biswajit Guchhait, and Ranjit Biswas*

Department of Chemical, Biological and Macromolecular Sciences, S. N. Bose National Centre for Basic Sciences, JD Block, Sector III, Salt Lake City, Kolkata 700 098, India

Supporting Information

ABSTRACT: In this paper, we explore the effects of the chain length of simple monohydroxy alcohol (C_nOH, $2 \leq n \leq 8$) and benzyl alcohol ($C_6H_5CH_2OH$) upon the fluorescence dynamics of a dipolar solute probe, coumarin 153 (C153), in vesicles formed in aqueous solutions of two oppositely charged (cationic and anionic) surfactants in the presence of 0.05 mol kg^{-1} alcohol. The catanionic vesicles are composed of 70 mol % sodium dodecyl sulfate (SDS) and 30 mol % cetyltrimethylammonium bromide (CTAB). The presence of alcohols of different chain length improves the stability of the catanionic vesicles. Dynamic light scattering (DLS) experiments suggest a gentle increase in the hydrodynamic diameter of the catanionic vesicle with alcohol chain length up to $n = 4$ and then an abrupt increase for the rest of the alcohols considered. The polarity and dynamics of the catanionic vesicles, probed by the steady-state and time-resolved fluorescence spectroscopy, indicate a signature of confined water. Quantities measured from fluorescence experiments of these vesicles also show a mild variation for alcohols of chain length $n \leq 4$, followed by a sudden variation for alcohols with $n > 4$. Interestingly, pentanol and benzyl alcohol in catanionic vesicles showed roughly similar effects due to their equivalent chain length. All of these data are remarkably correlated with the recently observed depression of the solubility temperature of catanionics with alcohol chain length (*Langmuir* **2009**, *25*, 12516−12521).

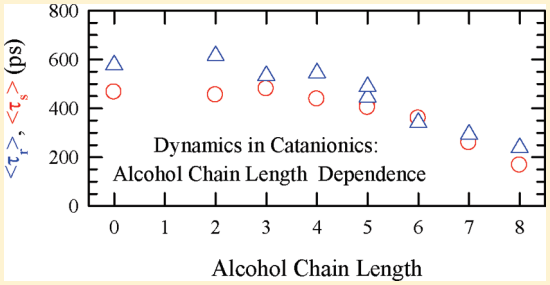

I. INTRODUCTION

Catanionics, a mixture of anionic and cationic surfactants self-organized in aqueous solutions, exhibit properties which are different from the corresponding properties of the individual surfactants.[1−5] The presence of different kinds of molecular interactions in such solutions of surfactant mixture leads to formation of microstructures. Addition of straight-chain alcohols (C_nOH with $2 \leq n \leq 8$) to catanionic solution leads to formation of aggregates of different shape and size, such as, spherical and rodlike micelles, vesicles, and so on. The straight chain alcohols (hereafter simply "alcohols") with $n \geq 4$ favor the formation of vesicles.[6−8] The first experimental example of the vesicle of biological importance was reported in 1965,[9] and since then many practical applications followed. Surfactants and their mixtures well above their critical micelle concentrations (CMCs) are good examples of biological cell membranes.[9−13] Over the years surfactant mixtures have attracted attention because the mixtures of oppositely charged surfactants, either both double-chained and single-chained or single- and double-chained surfactants in aqueous medium produce vesicles.[5,14−28] Synthetic vesicles resembling the biological membranes have been prepared using double-chain phospholipids for understanding the biological processes.[29] Catanionics made of a mixture of an anionic and a cationic surfactants at 1:1 molar ratio tend to precipitate.[15,30,31] However, tuning the molar ratio of one of the surfactants and keeping the total surfactant concentration ∼1−2 wt %, the catanionic mixtures can lead to formation of vesicles.[23,32] This is mainly due to favorable thermodynamics[33] and packing of the polar headgroup.[10,34,35] Catanionic vesicles are potential candidates for their applications in biology, pharmaceutical industry, and nanoreactors[36−45] and are being investigated experimentally and theoretically to use them as models for biological membranes.[23,28,33,46−52]

Though single-chain anionic and cationic surfactant mixtures with excess mole fraction of one of the surfactants in aqueous medium form vesicles on solubilization, they are not thermodynamically stable and precipitation appears after some time. However, the stability of the catanionic vesicles can be improved by adding alcohols.[52,53] Within the solubility limit of the alcohol concentration in such mixtures the stabilities of catanionic

Received: February 12, 2011
Revised: May 31, 2011
Published: June 17, 2011

Scheme 1. Schematic Representation of a Vesicle (Shape Considered To Be Spherical) Showing Various Regions[a]

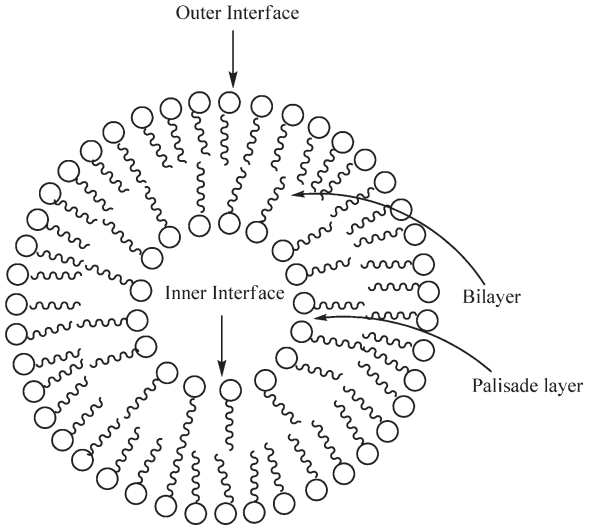

[a] "Inner Interface" means interface created between the self-assembled charged headgroups (circles) and confined solvent molecules (not shown for clarity), and "Outer Interface" indicates an interface between the charged headgroups and bulk solvent molecules. "Bilayer" is formed via the assembly of the surfactant tails (shown by chains). For a more informative discussion, please see ref 35.

vesicles are increased by using alcohols (C_1OH to C_8OH) and follow the order $C_1OH < C_2OH < C_3OH < C_4OH < C_5OH < C_6OH < C_7OH < C_8OH$.[6−8,53−57] Recently, a remarkable correlation has been observed between the solubility temperature depression of the catanionics and the chain length of the alcohol used.[53] In addition, an interesting analogy is observed between the alcohol effects on the solubility pattern of the catanionics and the anesthetic potency of these alcohols on tadpoles.[53]

There are experimental and theoretical evidence that alcohols behave like a cosolvent and cosurfactant, depending on the chain length and concentration.[58,59] It was found that alcohols with $1 \leq n \leq 3$ at low concentrations are incorporated in the micellar structure and, at higher concentration, reside primarily in the aqueous phase.[58] In contrast, alcohols having $4 \leq n \leq 7$ are primarily incorporated in the micellar structure exhibiting cosurfactant property.[59] These observations regarding the location of added alcohol molecules are important for interpreting data obtained from fluorescence spectroscopic experiments of aqueous solutions containing catanionic vesicles stabilized by alcohols. Water molecules present in such solutions could be broadly divided into three types (see Scheme 1): bulk water molecules, water molecules which are near the charged headgroups at the outer periphery, and water molecules inside the core. It is now known from numerous studies that water molecules which reside near the charge headgroups (in the present scenario water molecules both near the outer and inner peripheries which could be termed as "interface" water) are responsible for much slowed-down dynamics compared to that of bulk water.[60−84] A recent report on solvation dynamics in catanionic vesicles composed of 62.5 wt % SDS and 37.5 wt % dodecyltrimethylammonium bromide (DTAB) in aqueous medium without alcohol indicates much faster medium dynamics than in aqueous micelles.[50] This suggests a critical role of bulk water in determining the rate of solvation energy relaxation of a laser-excited dye dissolved in an aqueous medium containing vesicles.

The bilayer composed of hydrophobic chains of the surfactants[85] can easily accommodate the alcohols, particularly the longer chained ones, via the favorable hydrophobic interactions. The possibility of water molecules buried in the bilayer is nonexistent as comparative experimental studies with lipids and structurally simpler surfactants have demonstrated the absence of water molecules buried by the alkyl chains of the surfactant molecules.[86−88] Alcohols, such as pentanol and hexanol, at low concentration in SDS micelles, on the other hand, have been found to reside at the palisade layer and, at higher concentrations, mainly stayed in the micellar interior with a small fraction in the palisade layer.[89,90] But alcohols with $7 \leq n \leq 10$ reside mainly in the hydrophobic chain region leading to an increase in micellar aggregate size.[90] This information regarding locations of the water and alcohol molecules has important bearing on attributing the fluorescence response observed in alcohol-stabilized aqueous catanionic vesicles to probe−water interactions alone as the fluorescent probes used in this study are soluble in both nonpolar and polar solvents.[91]

Considering the above facts, in the present paper we have focused our attention on unraveling the effects of alcohols (ethanol to octanol) and benzyl alcohol at a fixed concentration in the mixture of surfactants (SDS + CTAB) on the medium structure and dynamics using two nonreactive fluorescent probes (pyrene and coumarin 153). Addition of alcohols imparts heterogeneity in the surfactant mixture in the microscopic level forming vesicles and micelles with different shapes and sizes. Our dynamic light scattering study reveals a sudden increase in the hydrodynamic diameter of vesicles as the alcohol changed from pentanol to hexanol, a point at which the polydispersity index has also been found to change its slope. The solvents (here water and alcohol) are expected to behave differently because of the complex interactions that they experience with the surrounding environment. Solvents residing within the vesicle are different from that present in the bulk with respect to polarity and viscosity. While steady-state fluorescence experiments reveal the change in polarity of the medium, time-resolved measurements reflect on modifications in both medium polarity and stiffness. Spectral width, ratio between band intensities, and average solvation and rotation times measured using fluorescent probes all show a sudden change in chain length dependence as butanol is replaced by its higher analogue. All of these fluorescence spectroscopic results exhibit a strong correlation with the alcohol chain length dependence of solubility temperature for these complex systems in the presence of 0.05 mol kg^{-1} alcohol.

II. EXPERIMENTAL SECTION

IIa. Materials. SDS (≥99%, SRL), CTAB (98%, Alfa Aesar), ethanol (99.7−100%, BDH), *n*-propanol (+99%, Acros), *n*-butanol (99%, Acros), *n*-pentanol (99%, Acros), *n*-hexanol (98%, Acros), *n*-heptanol (98%, Acros) *n*-octanol (99%, Acros), benzyl alcohol (99%, Qualigens Fine Chemicals), pyrene (>97%, Fluka), and coumarin 153 (Exciton) were used as received. Double-distilled water was used to prepare the solutions.

IIb. Preparation of Catanionic Vesicles. A suspension of (70 mol % SDS + 30 mol % CTAB) catanionics in double-distilled water was prepared keeping the total surfactant concentration at 1 wt % and was stirred to ensure homogeneous suspension. Approximately 8 mL of the suspension was transferred to a series

of preweighed screw-capped sample tubes, and the final weights were taken. To these suspensions, different amounts of alcohols (C_2OH-C_8OH) and $C_6H_5CH_2OH$ were added to maintain a constant concentration of 0.05 mol kg^{-1} alcohol. The details are given in ref 53. Note that even though the stability depends on the chain length of alcohols,[53] all of the solutions are stable enough for carrying out the measurements.

IIc. Conductivity Measurements. The specific conductivities of the catanionic vesicles were measured with a dip-type cell having a cell constant of 114.1 m^{-1} and a LCR bridge (model 6440A, Wayne Kerr) at 298 K as a function of alcohol chain lengths.

IId. Dynamic Light Scattering Measurements. The hydrodynamic diameters of catanionic vesicles as a function of alcohol chain length were measured by using the dynamic light scattering (DLS) technique with a Zeta Sizer 3000HS (Malvern) employing a 5 mW He−Ne laser with wavelength output of 632.8 nm. The scattering angle was 90°, and the scattering intensity data were processed using the software supplied with the instrument to obtain the hydrodynamic diameter. All measurements were made at 298 K.

IIe. Spectroscopic Experiments. The fluorescence emission spectra of pyrene were recorded on a fluorescence spectrophotometer, F4500, (Hitachi) at 298 K. The excitation wavelength of pyrene was 335 nm, and the excitation and emission slits were kept constant at 10 and 2.5 nm, respectively. The fluorescence emission was recorded in the range of 350−420 nm. From the spectra, the ratio of intensities of the first and the third vibrational peaks of pyrene, I_1/I_3, was calculated. Pyrene concentration in the solutions containing catanionic vesicles was kept fixed at ~1.5 μM.

The details of the solvation dynamics and the fluorescence anisotropy could be found elsewhere.[81] Briefly, the steady-state absorption (Shimadzu UV-2450) and emission spectra were recorded in a spectrophotometer and a Jobin-Yvon Fluoromax-3 fluorimeter, respectively. The probe, C153 was added to the catanionics mixtures, the concentration of the probe was $\leq 10^{-5}$ M, and the samples were placed in a cuvette of 1 cm path length. The emission was collected via time-correlated single-photon counting (TCSPC) for 18−20 wavelengths across the steady-state emission spectrum of C153 for a given sample at a fixed excitation wavelength of 409 nm. The typical full width at half-maximum (fwhm) of the instrument response function (IRF) with this excitation source was ~75 ps. The solvation dynamics in these solutions was followed by monitoring the peak shift in the time-resolved emission spectrum (TRES)[91] of C153. The solvation dynamics is described by the solvation response function,[91] $S(t) = (\nu(t) - \nu(\infty))/(\nu(0) - \nu(\infty))$, where $\nu(0)$, $\nu(t)$, and $\nu(\infty)$ are the emission maxima (frequencies) at times 0, t, and ∞, respectively. Subsequently the average solvation time, $\langle\tau_s\rangle$, was determined from the amplitudes (a_i) and time constants (τ_i) obtained from multiexponential fit to the measured $S(t)$ as follows,

$$\langle\tau_s\rangle = \int_0^\infty dt\, S(t) = \int_0^\infty dt\, [a_i \exp(-t/\tau_i)] = \sum_i a_i\tau_i, \quad \text{with} \sum_i a_i = 1 \tag{1}$$

The fluorescence anisotropy decay of the same probe (C153) was monitored at the peak wavelength of the steady-state emission bands so as to minimize the effects of fast decay or rise due to solvent reorganization.[92] As usual, the time-resolved fluorescence anisotropy, $r(t)$, was constructed from the collected time-dependent parallel ($I_{\parallel}(t)$) and perpendicular ($I_{\perp}(t)$) fluorescence intensity decays as follows,[92]

$$r(t) = \frac{I_{\parallel}(t) - GI_{\perp}(t)}{I_{\parallel}(t) + 2GI_{\perp}(t)} \tag{2}$$

where G accounts for the differential sensitivity to the two polarizations, which was obtained by tail matching. The average value for G was found to be 1.15 ± 0.05.

The constructed $r(t)$ was first deconvoluted from the IRF and then fitted to a biexponential function using an iterative reconvolution-fitting program.[92] The following biexponential function of time was used,

$$r(t) = r(0)[a_1 \exp(-t/\tau_1) + (1 - a_1)\exp(-t/\tau_2)] \tag{3}$$

where τ_i (i = 1, 2) represents the time constants for the decay components (a_i). The value for the initial anisotropy, $r(0)$, was fixed at 0.376 while fitting the $r(t)$ for C153 in all the solutions studied here.[92] The average rotational correlation time, $\langle\tau_r\rangle$, was then determined as follows: $\langle\tau_r\rangle = \int_0^\infty dt\, [r(t)/r(0)] = a_1\tau_1 + (1 - a_1)\tau_2$.

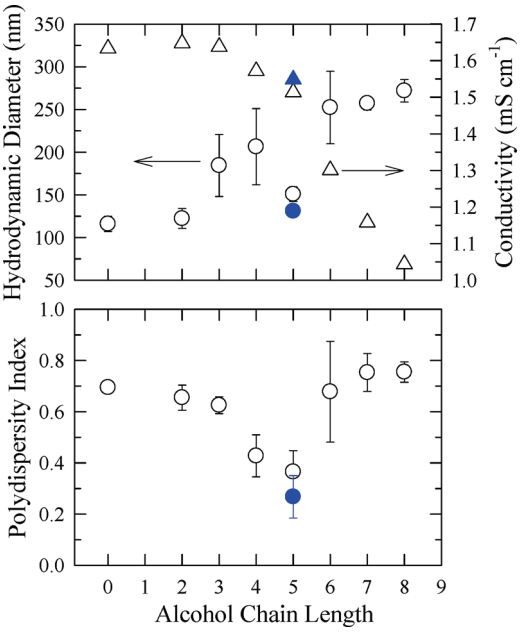

Figure 1. Plots of hydrodynamic radius and specific conductivity (upper panel) and polydispersity index (lower panel) vs chain length of alcohols. Closed symbol represents benzyl alcohol and open symbols represent *n*-alcohols.

III. RESULTS AND DISCUSSION

IIIa. Hydrodynamic Diameter and Specific Conductivity. The (70 mol % SDS + 30 mol % CTAB) catanionic without and with alcohols (C_2OH-C_8OH) and benzyl alcohol at 0.05 mol kg^{-1} on solubilization yield bluish solutions, which indicate the formation of large particles consisting of vesicles and micelles. The progressive increase in the chain length of the alcohol has a distinct contribution on the hydrodynamic diameter and the polydispersity index of the vesicles and micelles so formed (Figure 1). The polydispersity index (PDI) pattern (Figure 1,

lower panel) indicates that (70 mol % SDS + 30 mol % CTAB) catanionic which corresponds to (22.5 mM SDS and 9.64 mM CTAB) alone and with alcohols produce primarily vesicles and rodlike micelles.[93] Note PDI suggests a size distribution of particles in the catanionics, and a value close to unity indicates domination of particles of uniform size. A value for the PDI between 0.2 and 0.7, on the other hand, suggests a wider size distribution.[54,94] For catanionics containing alcohols with $n > 5$, particle size is large as indicated by the corresponding hydrodynamic diameter (upper panel, Figure 1). For catanionics containing alcohols with $n < 5$, probably different kinds of particles (for example, vesicles and rodlike micelles) populate the mixture. Interestingly, transmission electron microscopic (TEM) experiments have shown that aqueous mixtures of surfactants with compositions (10 mM SDS + 0.1 mM CTAB) and (0.03 mM SDS + 10 mM CTAB) produce mixed micelles with ~50 nm average diameter.[94] The (70 mol % SDS + 30 mol % DTAB) catanionic without any additive produces a micelle with R_H= 10 nm.[95] Note that the (64 mol % SDS + 36 mol % DTAB) catanionic yields a vesicle with ~400 nm diameter.[22,50] These results seem to suggest that the composition and the identity of surfactant pairs are governing factors for micelle and vesicle formation.

It is interesting to note that catanionics with pentanol ($n = 5$) and benzyl alcohol demarcate the solubility pattern of these mixtures as a function of alcohol chain length at 0.05 mol kg^{-1} alcohol.[53] The distribution of large particles in catanionics for alcohol with $n = 5$ is narrow and occupied mainly by vesicles. Earlier we demonstrated that the chain length of the alcohol at a fixed concentration greatly influences the solubility temperature of (70 mol % SDS + 30 mol % CTAB) catanionics.[53] Similar effects were observed by using an aromatic alcohol of equivalent chain length.[53] The DLS results presented here also reflect the same correlation. It was observed that alcohols with $n = 2$ and 3 at 0.05 mol kg^{-1} do not decrease the solubility temperature of neat (70 mol % SDS + 30 mol % CTAB) catanionic (312.5 ± 0.1 K) but alcohols with n ranging between 4 and 8 significantly decrease the solubility temperature. Note that the geometry of the catanionic vesicles and the core size in the presence of alcohols with different chain lengths are likely to be different with different polarity. This is because of (i) alignment of alcohol in the bilayer according to the dielectric constant of the medium,[54,96] (ii) cosolvent and cosurfactant characters of alcohols,[56,58,59] and (iii) the signature of the alcohol in the packing parameter.[10,34,35]

The diameter of the catanionic vesicles increases with the increase in chain length of alcohols at a fixed concentration. This observation is not surprising. Because of higher solubility of short-chain alcohols ($1 \le n \le 3$) in water, only fewer ethanol and propanol molecules enter the assemblies[56,58,59,96,97] and reside mainly in the layer close to the surfactant headgroups[6] making the packing parameter optimum for vesicle formation. Consequently, the size of the particles remains almost constant (Figure 1, upper panel). Alcohols with $n \ge 4$ probably enter into the assemblies to a larger extent and increase the area of the headgroup, causing an increase in the hydrodynamic diameter of the vesicles and micelles. This also enhances the hydrophobicity in the tail (bilayer) region. Available results suggest the following sequence of the hydrodynamic diameter of the vesicle at 0.05 mol kg^{-1} alcohol: C_0 (no alcohol) ≈ $C_2 < C_3 < C_4 < C_5 < C_6 < C_7 < C_8$. Note the present results are in tune with the results of SDS micelles,[98] but no leveling-off at C_8 is realized as it was observed in the solubility temperature.[53]

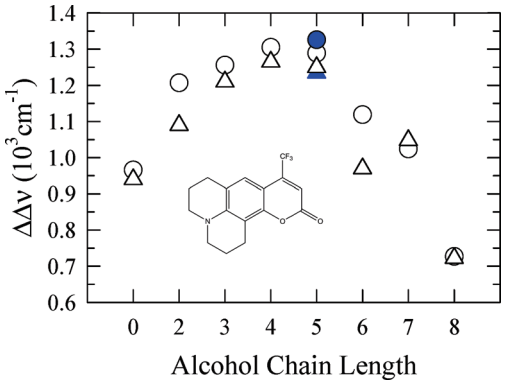

Figure 2. Alcohol chain length dependence of relative Stokes' shift ($\Delta\Delta\nu$) measured using C153 as a probe in these catanionics. The blue circle represents $\Delta\Delta\nu$ when the added alcohol is benzyl alcohol. The alcohol concentration is 0.05 mol/kg. The second data set indicates reproducibility. The chemical structure of C153 is also shown inside the figure.

The specific conductivity (κ) of charge carriers in a dielectric medium is represented by $\kappa = \Sigma\rho_i|z_i|e\mu_i$, where ρ_i is the number density of the ith charged particle, $|z_i|e$ the charge of the particle, and μ_i the mobility of the charged particle. We presume that the catanionic vesicles formed without and with alcohol have roughly the same number density with similar charge. In addition, our measurements (results not shown here) indicate the ζ potential is negative for all of the catanionic vesicles reported in this study. In that case the specific conductivity is largely dependent on the mobility vis-à-vis the size of the vesicle. The specific conductivities of the catanionic vesicles without and with alcohol up to $n = 3$ are roughly constant due to comparable diameter (Figure 1, upper panel). But the specific conductivity decreases with chain length after $n \ge 4$ and in accordance with the increase in hydrodynamic diameter (Figure 1). These results therefore demonstrate that the mobility of particles and the average dielectric constant (ε_0) of the medium in the absence and presence of alcohols up to $n = 3$ are roughly equal, and the alcohols probably behave like a cosolvent. For alcohols with $n \ge 4$, the mobility decreases as the size (hydrodynamic diameter) of the moving body increases due to the penetration of higher alcohols into the hydrophobic layer. This manifests the ability of higher alcohols to behave as cosurfactant.[56]

IIIb. Steady-State Spectral Properties. Figure 2 presents the relative Stokes' shift ($\Delta\Delta\nu$) for C153 as a function of alcohol chain length calculated from the peak frequencies of the absorption (ν_{abs}) and emission (ν_{em}) spectra as follows: $\Delta\Delta\nu = [\nu_{abs} - \nu_{em}]^{sample} - \Delta\nu^{np}$, where $\Delta\nu^{np}$ denotes the Stokes' shift value for the same probe in a nonpolar reference solvent at that temperature. Representative absorption and emission spectra are shown in Figure S1 (Supporting Information). We have used 2-methylbutane (2-MB) as a nonpolar reference for which $\Delta\nu^{np}$ has been found to be 4390 cm^{-1}. These data clearly indicate a nonmonotonic dependence of $\Delta\Delta\nu$ on alcohol chain length (n) with a peak at $n = 5$. Strikingly, when one uses benzyl alcohol, the value for $\Delta\Delta\nu$ (shown by a blue circle) becomes comparable to those found for pentanol. The observed nonmonotonic dependence of $\Delta\Delta\nu$ originates mainly from the nonmonotonic dependence on chain length of the absorption peak frequency (ν_{abs}) of C153 in these solutions containing vesicles as the corresponding emission frequencies (ν_{em}) show an almost linear dependence. Figure S2 (Supporting Information) demonstrates

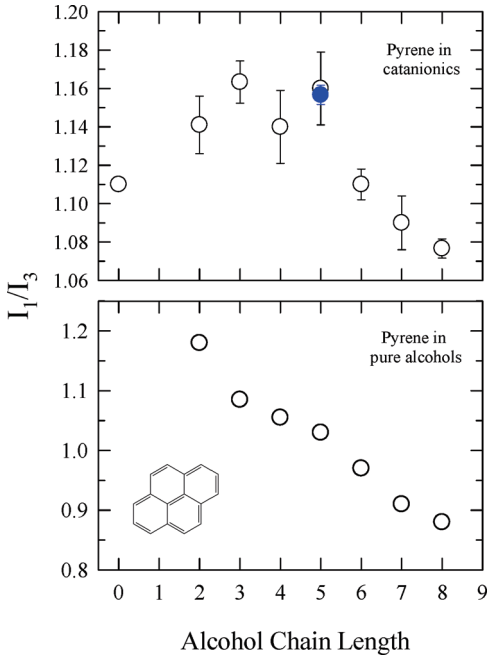

Figure 3. Variation of I_1/I_3 of pyrene in catanionics in the absence and presence of alcohols. Closed symbol represents benzyl alcohol, and open symbols represent *n*-alcohols. The lower panel depicts I_1/I_3 of pyrene in pure *n*-alcohols. The chemical structure of pyrene is also shown.

this fact. However, the emission spectral width, Γ_{em} (lower panel, Figure S2), exhibits a change in slope in its chain length dependence at C_4 even though the total variation in Γ_{em} is only about 200 cm^{-1}. Interestingly, all of these steady-state spectral data follow the alcohol chain length sequence observed earlier in the depression of the solubility temperature.[53]

IIIc. Polarity of the Catanionics Vesicles. The polarity of the catanionic mixtures in the absence and presence of 0.05 mol kg^{-1} alcohols and benzyl alcohol has been examined through pyrene fluorescence emission spectrum and is shown in the upper panel of Figure 3. It is interesting to note that the polarity of the catanionic vesicles remains nearly constant for $1 \leq n \leq 4$ and then decreases gradually with *n*. The value of I_1/I_3 for the catanionic mixture in the absence of any added alcohol is ~1.10 and thus in semiquantitative agreement with the reported value.[52] Note I_1/I_3 for catanionics in the presence of alcohols with $1 \leq n \leq 4$ is nearly constant (1.15 ± 0.1) and different from that observed for aqueous solution of pyrene (1.56),[99] aqueous micelles formed by CTAB (1.30),[99] and SDS (1.14)[100] but agrees well with that for ethanol (Figure 3, lower panel). The intensity ratio (I_1/I_3) in catanionic vesicles further decreases to ~1.06 for octanol ($n = 8$) but still is much larger than the value (~0.60) for pyrene in alkane of comparable chain length.[99] This comparison suggests that pyrene in these catanionics in the presence of alcohol is not exclusively located in the hydrophobic zone made by the surfactant tails. This observation and the results obtained for pure alcohols therefore indicate pyrene is located mainly at the micellar interface where the higher chain alcohols increasingly replace water molecules to solvate the charged headgroups. The decrease in average dielectric constant (ε_0) with chain length for these alcohols is well-known, and thus the decrease in intensity ratio indicates the presence of alcohols in the environment surrounding pyrene. This also reflects the cosolvent

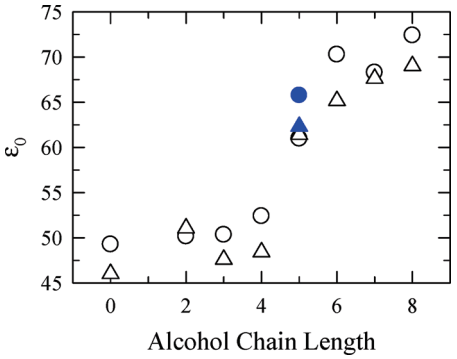

Figure 4. Alcohol chain length dependence of estimated dielectric constant (ε_0) of the catanionic vesicles. The blue circle represents the estimated ε_0 in the presence of benzyl alcohol. Repeat measurements are also shown in order to indicate reproducibility.

property of higher alcohols[56] for these catanionic systems. For short-chain alcohols ($2 \leq n \leq 4$) which are highly soluble in water, it is likely that at such a low concentration these alcohols in catanionic mixtures will largely be localized in the aqueous phase.[6,56,98] Since clustering of alcohol molecules occurs in very dilute aqueous binary mixtures and the size of the clusters depends on temperature and alcohol chain length,[101−107] pyrene could selectively reside in those clusters. This probably explains the increase in I_1/I_3 ratio with chain length for short-chain alcohols in these catanionics. As noted earlier,[108,109] these results imply that pyrene, being a strongly hydrophobic molecule and possessing a non-dipolar ground state, does not penetrate into the confined polar solvent pool inside the vesicles. Consequently, it remains insensitive to the changes in the polarity of the confined polar pool due to the change in hydrodynamic radius of the vesicles with alcohol chain length.

IIId. Estimation of the Average ε_0 of the Confined Polar Pool Inside the Catanionic Vesicles. Subsequently, C153—a polarity probe, which possesses a large dipole moment in both ground and excited states[91]—has been employed to estimate the average dielectric constant of the confined aqueous pool inside these vesicles in the presence of 0.05 mol kg^{-1} alcohol. As before,[110,111] insertion of the measured fluorescence emission peak frequencies (ν_{em} in 10^3 cm^{-1}) and subsequent inversion of the following empirical relation

$$\nu_{em} = \nu_g^{em} - A[(\varepsilon_0 - 1)/(\varepsilon_0 + 2)] - B[(n^2 - 1)/(n^2 + 2)] \quad (4)$$

produces the estimated ε_0 shown in Figure 4 as a function of alcohol chain length for these catanionic mixtures. While determining ε_0 values from eq 4, we have used (all in proper units) $\nu_g^{em} = 23.12$, $A = 5.06$, and $B = 1.5$ and assumed a value for the refractive index (n) as that of pure bulk water (1.33). It is evident from this figure that the estimated ε_0 values of the polar pool vary in the range between ~50 and ~70. Interestingly, estimated ε_0 for the micelle−water interface in aqueous micelles of sodium laurate and sodium lauryl sulfate was found to lie between ~40 and ~45.[99] It is important to mention here that the total shift in the measured ν_{em} is less than 200 cm^{-1} in which the ion−dipole interaction between the charged particles (headgroups and counter ions) and C153, in addition to dipole−dipole solute−solvent interaction, also contribute. Thus, the estimated ε_0 might not be an accurate representation of confined solvent

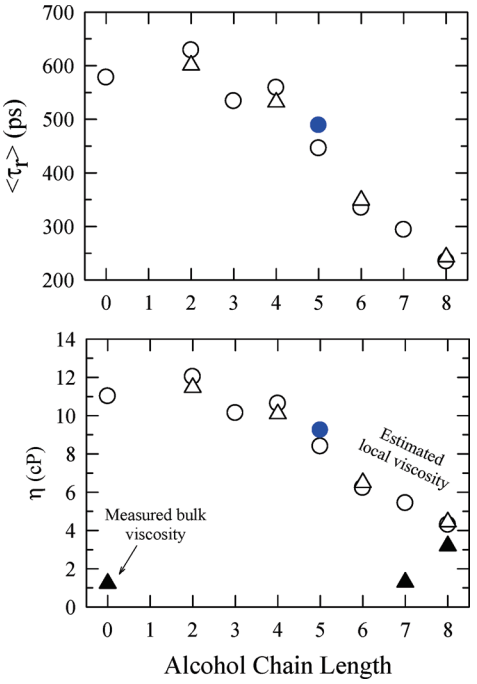

Figure 5. Alcohol chain length dependencies of average rotation time ($\langle\tau_r\rangle$) for C153 in these catanionics (upper panel) and local viscosity (η, lower panel) estimated from $\langle\tau_r\rangle$. Filled triangles (lower panel) represent measured bulk solution viscosity of these catanionics at a few representative alcohol chain lengths. Repeat measurements for a few (representative) chain lengths are also shown.

polarity but rather only a qualitative picture of the average polarity surrounding the solute at the interface (formed between the surfactant headgroups and confined water molecules inside catanionic vesicles). Given the large solubility of C153 in alcohols, a possibility of C153 being partitioned into the bulk aqueous phase always exists, particularly when the added alcohols are short-chain ones. C153, being sparingly soluble in water and strongly polar in its ground state itself, a combination of ion−dipole (surfactant headgroup−solute) and dipole−dipole (solvent−solute) interactions drives probably most of the solute population inside the vesicle and then pulled up near the headgroup−water interface via interaction sorting. The decrease in average polarity exhibited by pyrene with alcohol chain length and quite the opposite by C153 strongly suggest that the latter (C153) is trapped inside the polar solvent pool of the vesicles formed in the aqueous solutions of surfactant mixtures in the presence of alcohols.

If the above picture is qualitatively correct, then the alcohol chain length dependent estimated ε_0 depicted in Figure 4 bears the following meaning. Since the hydrodynamic diameter of these catanionic vesicles is ≥100 nm, estimated $\varepsilon_0 \geq 50$ is only expected from our earlier work.[111] A weak dependence of ε_0 on the chain length for short-chain alcohols (from ethanol to butanol) follows from the fact that these alcohols largely act as cosolvent and do not greatly influence the size of the vesicles. The slow change in both hydrodynamic radius and conductivity shown in Figure 1 in this regime nicely fits into this picture. For pentanol and higher alcohols ($n \geq 5$), the cosurfactant property of the alcohol dominates, causing an increase in the pool size. This is sensed by the encapsulated fluorophore and reflected in the increase of ε_0. The change in estimated ε_0 in this regime also corroborates well with the corresponding diameter and conductivity data. Strikingly, the estimated ε_0 becomes almost comparable to that of bulk water ($\varepsilon_0 \sim 78$ at 298 K) at the largest confinement (*diameter* ∼ 260 nm). This seems to support the common understanding that confinement-induced effect on bulk dielectric constant becomes negligible at sufficiently large confinement. However, how large is large enough for allowing the trapped solute to sense the "bulk" polarity is a question of further investigation, and a realistic simulation study may be able to answer such a question.

IIIe. Rotational Dynamics and Estimation of Local Viscosity. Next we present the average rotational correlation times in the catanionic vesicles in the presence of varying alcohol chain length. The decay of the time-resolved fluorescence anisotropy, $r(t)$, for C153 in the catanionic vesicles has been found to be a biexponential function of time, irrespective of the chain length of the alcohol used. While a few (representative) fluorescence anisotropy decays are shown in Figure S3, biexponential fit parameters describing the $r(t)$ decays are provided in Table S4 (Supporting Information). The $\langle\tau_r\rangle$ obtained from the collected decays are shown in the upper panel of Figure 5 as a function of alcohol chain length. Note in this figure that $\langle\tau_r\rangle$ remains largely insensitive to the identity of the alcohol up to butanol and then shows a sudden fall as chain length is increased. In addition, $\langle\tau_r\rangle$ in the presence of benzyl alcohol is comparable to that measured for pentanol. All of these results are quite similar to the trend observed for variation in solubility temperature with alcohol chain length for these catanionics in the presence of 0.05 mol kg^{-1} alcohol. The measured biphasic anisotropic decays consist of a fast component (∼50−70%) with time constant ranging between ∼40 and 80 ps and a slow component whose time constant varies between ∼700 and ∼1400 ps. Earlier measurements with C153 in catanionic aqueous reverse micelles of SDS and DTAB [81] also indicated a similar fast component with time constant ≤ 40 ps and a slow component with time constant ≤ 500 ps. Interestingly, these decay parameters strongly resemble those for C153 in pure pentanol ($T = 295 \pm 2$ K) where $\langle\tau_r\rangle$ was found to be ∼240 ps.[92] In the present study a similar value for $\langle\tau_r\rangle$ has been obtained in the presence of octanol, suggesting that the local environment around the probe in this particular catanionic vesicle is, on an average, similar to that in pure pentanol.

The above consideration of local environment motivated us to estimate the local viscosity from the anisotropy data and compare with the bulk viscosities of pure solvents and aqueous solutions of these catanionics in the presence of alcohols. The local viscosity experienced by the probe has been estimated by using the correlation, $\langle\tau_r\rangle = (58.1 \pm 1.6)\eta^{0.96\pm0.03}$, constructed from the rotation data of the same probe in bulk polar protic and aprotic solvents at room temperature.[92] Note that $\langle\tau_r\rangle$ is in picosecond (ps) and η is in centipoise (cP). The results are shown as a function of alcohol chain length in the lower panel of Figure 5, where, for comparison, the measured bulk viscosities[112] of aqueous solutions of the catanionics in the presence of 0.05 mol kg^{-1} alcohol are also presented. The pattern of decrease in η with alcohol chain length is expected because of the chain length dependency of $\langle\tau_r\rangle$, but what is more interesting is the fact that the estimated local viscosities are uniformly larger than the measured bulk solution viscosities. In fact, in the absence of any alcohol the estimated local viscosity is almost an order of magnitude larger than the corresponding bulk solution viscosity. This provides further evidence in favor of the assumption that

Table 1. Alcohol Chain Length Dependent Dynamic Stokes' Shift and Fit Parameters Describing Solvation Response Functions Measured Using C153 in Catanionics at∼298 K in the Presence of 0.05 *m* Alcohol

alcohol chain length	observed shift (cm^{-1})	"true" shift (cm^{-1})	% detected	a_1 (%)	τ_1 (ps)	a_2 (%)	τ_2 (ps)
0 [a]	856	2173	39	22	149	78	556
2	902	2265	40	24	59	76	556
3	838	2044	41	25	154	75	588
4	763	1981	39	16	93	84	500
5	890	2474	36	100	417		
BA [b]	961	2206	44	14	91	86	456
6	868	2401	36	19	110	81	430
7	1202	2243	54	22	52	78	323
8	1552	2378	65	56	49	44	313

[a] "0" indicates the absence of any added alcohol. [b] "BA" represents benzyl alcohol.

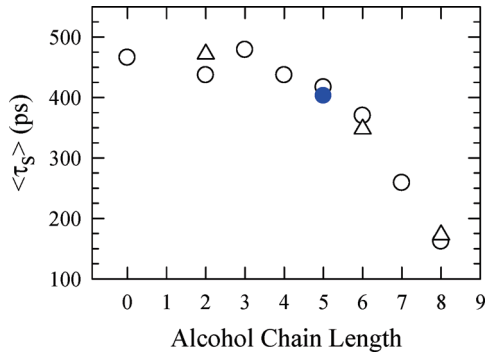

Figure 6. Alcohol chain length dependence of average solvation time ($\langle\tau_s\rangle$) for C153 in these catanionics. Datum in the presence of benzyl alcohol is represented by the blue circle. Multiple data at a few alcohol chain lengths represent reproducibility of the measurements.

C153 is residing inside the confined polar solvent pool of these vesicles. Note also that when the added alcohol is octanol, the local viscosity experienced by the trapped probe inside vesicles is numerically close to the bulk viscosity (3.51 cP)[92] of pentanol at ∼298 K, a direct consequence of $\langle\tau_r\rangle$ in these two media being very close to each other.

IIIf. Solvation Dynamics in Catanionic Vesicles. Table 1 summarizes the observed dynamic Stokes' shift values and estimated[113] "true" ones for C153 in the present catanionic vesicles. Time-resolved fluorescence decays at the blue and red wavelengths of the corresponding steady-state fluorescence emission spectrum of C153 at a few representative cases are shown in Figure S5 (Supporting Information). Decays at the blue wavelength and rise followed by decay at red wavelengths, as summarized in a table associated with Figure S5, indicate the presence of the dynamic Stokes shift in these catanionics. Data in Table 1 indicate that the true shift values for C153 range between ∼2000 and 2500 cm^{-1}, and the present experiments have missed approximately 40−70% of the true shift. Note the true shift values, particularly for bigger vesicle sizes, are somewhat larger than that measured for pure water (∼2000 cm^{-1}) using a structurally similar but water-soluble probe (C343).[114] The interaction between the solute and the charged headgroup (dipole−ion interaction) at the interface in addition to the water−solute (dipole−dipole) interaction[115−118] might be responsible for the excess shift over that measured for pure bulk water. Except for the system where pentanol is present,[119] all of the measured solvation response functions, $S(t)$, have been found to be biexponential with well-separated two time constants—one in the range of ∼50−150 ps (∼20−60%) and another in the range of ∼300−600 ps (∼40−80%). While these data are also provided in Table 1, fitted $S(t)$ decays for a few representative cases are shown in Figure S6 (Supporting Information). Note that biexponential dynamics has also been found earlier[120−123] in individual aqueous micellar solutions of SDS, CTAB, and Triton X-100 with short time constants very similar to those obtained here for the catanionics. Further investigation, using aqueous micelles of sodium alkyl sulfate (anionic) and alkyltrimethylammonium bromide (cationic) surfactants,[124] has revealed biexponential dynamics with the short time constant ranging between 110 and 160 ps. These results and the much shorter solvation time scales reported for bulk short-chain alcohols[91] strongly suggest that the current experiments have largely probed the solvation energy relaxation at the surfactant−polar solvent interface. Interestingly, the slow long time constants obtained for the present systems are similar to those observed for aqueous micellar solutions of alkyltrimethylammonium bromide but much slower than those reported for the aqueous micelles of sodium alkyl sulfate.[124] This might be regarded as an indirect evidence in favor of the fact that both the anionic and cationic surfactants participate in constituting the interface.

The time constants and amplitudes obtained from biexponential fits to the measured $S(t)$ are also summarized in Table 1. A close inspection of the tabulated time constants reveals a decrease with chain length for alcohols with $n > 4$ probably because of increased fluidity of the average environment around the solute at larger vesicle sizes. Note that the incomplete detection of the total dynamics can not only bias the detection toward slower dynamics, but it may also incorrectly put extra weight to the slower component. This can obscure the signature of distributed kinetics (stretched exponential) in such heterogeneous systems and make the dynamics appear as biexponential ones.[125] This limitation notwithstanding, the time constants do reflect a substantial alcohol chain length dependence, which becomes more evident when $\langle\tau_s\rangle$ are plotted as a function of alcohol chain length. This is depicted in Figure 6, where the datum corresponding to benzyl alcohol is also shown. Note in Figure 6 that $\langle\tau_s\rangle$, as found for the case of $\langle\tau_r\rangle$ in Figure 5, also exhibits a sudden change in alcohol chain length dependence around pentanol. In addition, $\langle\tau_s\rangle$ becomes comparable when the added alcohols are pentanol and benzyl alcohol. The similarity between the alcohol chain length dependence of $\langle\tau_s\rangle$ and $\langle\tau_r\rangle$ for

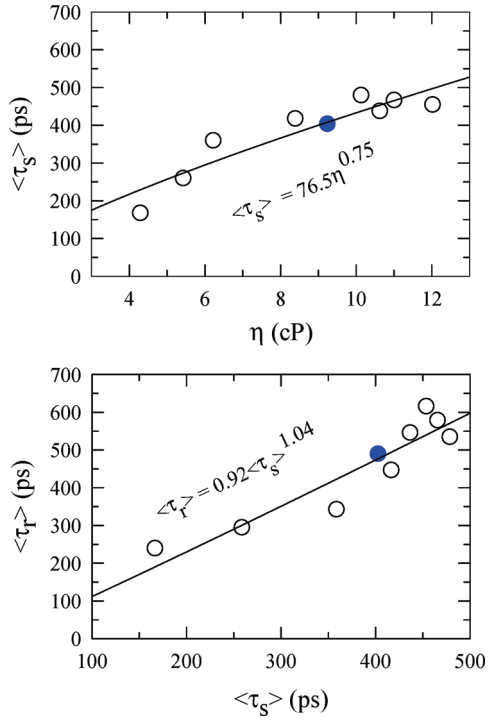

Figure 7. Dependence of average solvation time on estimated viscosity (upper panel) and correlation between the measured average solvation and rotation times (lower panel). Note $\langle\tau_r\rangle$ and $\langle\tau_s\rangle$ shown here are average of two sets shown in Figure 5 and Figure 6. The lines denote linear regression fits through the experimental data. In both cases, $R\sim 0.9$, R being the correlation coefficient.

C153 in these catanionic vesicles and that of solubility temperature therefore indicates a strong correlation between quantities accessed via time-resolved and thermodynamic measurements, which originates probably from the following common factor: the dominance of the cosurfactant property of the alcohols beyond butanol depresses solubility temperature but increases vesicle-size, leading to a less rigid average environment around a trapped solute making the movement of both the solute and solvent molecules more facile.

Since the average solvation and rotation times are governed by the rigidity of a given medium, these quantities could be used to explore the coupling between the solute and the immediate environment. Such an effort has led to a dependence of $\langle\tau_s\rangle$ on viscosity with a fraction power (that is, $\langle\tau_s\rangle \propto \eta^p$) and is depicted in the upper panel of Figure 7. The value of the fraction ($p = 0.75$) being less than unity is probably a reflection of the heterogeneous environment around the solute in such systems. While stating so, it should however be mentioned that such a conclusion here is based on a rather limited data set, and the local viscosity has not been independently measured but estimated via solute rotation. In addition, complete measurements of $S(t)$ are expected to reduce the numerical values of $\langle\tau_s\rangle$. However, the modified $\langle\tau_s\rangle$ will still be governed by the slowest time constant of the measured multiexponential $S(t)$ and, as a result, the correlation between $\langle\tau_s\rangle$ and η found here is expected to be preserved. Furthermore, the underlying frictional resistance regulating the rotation of a dissolved solute and its own solvation is likely to establish a correlation between $\langle\tau_r\rangle$ and $\langle\tau_s\rangle$. This is indeed the case as shown in the lower panel of Figure 7 where the interrelationship between $\langle\tau_r\rangle$ and $\langle\tau_s\rangle$ for C153 in these vesicles has been found to be as follows: $\langle\tau_r\rangle \geq 0.92\langle\tau_s\rangle^m$, with $m = 1.04$. Even though the approximate proportionality between $\langle\tau_r\rangle$ and $\langle\tau_s\rangle$ found here bears qualitative similarity to the observations in supercooled molten mixtures ($m = 1.09$)[115] and ionic liquids ($m = 1.03$),[126] the present results differ in the sense that while $\langle\tau_r\rangle/\langle\tau_s\rangle \approx 1$ for C153 in these vesicles, this ratio has been found to be ~5 for supercooled molten mixtures and ~9 for ionic liquids (except phosphonium ionic liquids). For phosphonium ionic liquids,[127] however, $\langle\tau_r\rangle/\langle\tau_s\rangle$ ranges between 2 and 3, which is comparatively much closer to the value found for these vesicles. While further investigation is required to establish whether a similar value of m signifies equivalent solute−solvent coupling in these widely different media, higher bulk viscosities of molten mixtures[128] and ionic liquids[129] are certainly responsible for the relatively larger values of $\langle\tau_r\rangle/\langle\tau_s\rangle$ in these media. Our very recent work[130] on dipolar solute rotation in polar liquids suggests that in highly viscous environment where the mechanical friction due to η exceeds that arising from the solute−solvent polarization coupling, $\langle\tau_r\rangle$ and $\langle\tau_s\rangle$ can show a linear interdependency. This theoretical analysis seems to explain the correlation between experimentally measured $\langle\tau_r\rangle$ and $\langle\tau_s\rangle$ for C153 in common solvents, molten mixtures, and ionic liquids.

IV. CONCLUSIONS

The influence of alcohols with different chain lengths and benzyl alcohol upon catanionic vesicles have been studied in 0.05 mol kg^{-1} alcohols. Our study demonstrates that alcohols with $n \geq 4$ act mainly as cosurfactants and enter the surfactant interface, increasing the size of the vesicles. The general trend of alcohols and benzyl alcohol upon the hydrodynamic diameter of the vesicles follows the order C_0 (no alcohol) $\approx C_2 < C_3 < C_4 < C_5 < C_6 < C_7 < C_8$. Both the average solvation and rotation times exhibit a sudden change in alcohol chain length dependence when the added alcohol is butanol. This result and others obtained from steady-state spectroscopic experiments are depicting the trend exhibited by the solubility temperature of these vesicle systems. Relevant fluorescence spectroscopic data indicate that while pyrene probes the outer interface between the surfactant headgroups and polar solvents, C153 enters into the confined solvent pool of these vesicles. In addition, average solvation times reported via fluorescence dynamics of C153 have been found to follow a fractional power-law dependence on estimated local viscosity. Like in ionic liquids and supercooled molten mixtures, average rotation and solvation times constitute a near-linear relationship between them.

■ ASSOCIATED CONTENT

Ⓢ Supporting Information. Figures showing representative absorption and florescence emission spectra of C153 in these catanionics, spectral frequencies and widths, anisotropy decays, fluorescence transients, and decays of solvation response function and tables listing anisotropy decay and fluorescence transient fit parameters. This information is available free of charge via the Internet at http://pubs.acs.org.

■ AUTHOR INFORMATION

Corresponding Authors

*E-mail: mahirrljt@yahoo.com (S.M.); ranjit@bose.res.in (R.B.).

■ ACKNOWLEDGMENT

S.M. is thankful to the Director, North-East Institute of Science & Technology, CSIR, Jorhat, India, for support and encouragement and thanks DAAD, Germany, for an equipment grant. S.M. is grateful to Prof. K. Ismail, Department of Chemistry, North-Eastern Hill University, Shillong, for providing a facility for recording pyrene fluorescence spectra. N.S. and B.G. are thankful to the CSIR, India, for research fellowships. H.A.R.G. thanks the Vice-Chancellor, Aliah University, West Bengal, for encouragement. We thank an anonymous reviewer for a careful reading of the manuscript and constructive criticism thereafter.

■ REFERENCES

(1) Lucassen-Reynders, E. H.; Lucassen, J.; Giles, D. *J. Colloid Interface Sci.* **1981**, *81*, 150.
(2) Li, G.-H.; Li, F.; Zheng, L.-Q.; Wang, H.-L. *Colloids Surf., A* **1993**, *76*, 257.
(3) You, Y.-L.; Hao, L.-S.; Nan, Y.-Q. *Colloids Surf., A* **2009**, *335*, 154.
(4) Zhu, B. Y.; Rosen, M. J. *J. Colloid Interface Sci.* **1984**, *99*, 435.
(5) Yatcilla, M. T.; Herrington, K. L.; Brasher, L. L.; Kaler, E. W.; Chiruvolu, S.; Zasadzinski, J. A. *J. Phys. Chem.* **1996**, *100*, 5874.
(6) Yu, W.-Y.; Yang, Y.-M.; Chang, C.-H. *Langmuir* **2005**, *21*, 6185.
(7) Zhang, X.-R.; Huang, J.-B.; Mao, M.; Tang, S.-H.; Zhu, B.-Y. *Colloid Polym. Sci.* **2001**, *279*, 1245.
(8) Wang, C.-Z.; Tang, S.-H.; Huang, J.-B.; Zhang, X.-R.; Fu, H.-L. *Colloid Polym. Sci.* **2002**, *280*, 770.
(9) Bangham, A. D.; Standish, M. M.; Watkins, J. C. *J. Mol. Biol.* **1965**, *13*, 238.
(10) Israelachvili, J. N. *Intermolecular and Surface Forces*; Academic Press: Orlando, FL, 1985.
(11) Evans, D. F.; Wennerström, H. *The Colloidal Domain: Where Physics, Chemistry, Biology, and Technology Meet*, 2nd ed.; Wiley-VCH: New York, 1999.
(12) Mahiuddin, S.; Renoncourt, A.; Bauduin, P.; Touraud, D.; Kunz, W. *Langmuir* **2005**, *21*, 5259.
(13) O'Driscoll, B. M. D.; Nickels, E. A.; Elder, K. J. *Chem. Commun. (Cambridge, U. K.)* **2007**, 1068.
(14) Marques, E.; Khan, A.; Miguel, M.; Lindman, B. *J. Phys. Chem.* **1993**, *97*, 4729.
(15) Kaler, E. W.; Murthy, A. K.; Rodriguez, B. E.; Zasadzinski, J. A. N. *Science* **1989**, *245*, 1371.
(16) Morgan, J. D.; Johnson, C. A.; Kaler, E. W. *Langmuir* **1997**, *13*, 6447.
(17) Iampietro, D. J.; Brasher, L. L.; Kaler, E. W.; Stradner, A.; Glatter, O. *J. Phys. Chem. B* **1998**, *102*, 3105.
(18) Brasher, L. L.; Herrington, K. L.; Kaler, E. W. *Langmuir* **1995**, *11*, 4267.
(19) Gonzáles, Y. I.; Stjerndahl, M.; Danino, D.; Kaler, E. W. *Langmuir* **2004**, *20*, 7053.
(20) Liu, S.; Gonzáles, Y. I.; Kaler, E. W. *Langmuir* **2003**, *19*, 10732.
(21) Kaler, E. W.; Herrington, K. L.; Murthy, A. K.; Zasadzinski, J. A. N. *J. Phys. Chem.* **1992**, *96*, 6698.
(22) Harrington, K. L.; Kaler, E. W.; Miller, D. D.; Zasadzinski, J. A. N.; Chiruvolu, S. *J. Phys. Chem.* **1993**, *97*, 13792.
(23) Tondre, C.; Caillet, C. *Adv. Colloid Interface Sci.* **2001**, *93*, 115.
(24) Brasher, L. L.; Kaler, E. W. *Langmuir* **1996**, *12*, 6270.
(25) Madani, H.; Kaler, E. W. *Langmuir* **1990**, *6*, 125.
(26) Iampietro, D. J.; Kaler, E. W. *Langmuir* **1999**, *15*, 8590.
(27) Raghavan, S. R.; Fritz, G.; Kaler, E. W. *Langmuir* **2002**, *18*, 3797.
(28) Marques, E. F.; Regev, O.; Khan, A.; Lindman, B. *Adv. Colloid Interface Sci.* **2003**, *100−102*, 83.
(29) Lasic, D. D.; Lipowskis, R.; Sackmann, E., Eds. *Handbook of Biological Physics*, Vol. 1; Elsevier Science B. V.: Amsterdam, 1995; Chapter 10.
(30) Horbaschek, K.; Hoffmann, H.; Hao, J. *J. Phys. Chem. B* **2000**, *104*, 2781.
(31) Stellner, K. L.; Amante, J. C.; Scamehorn, J. F.; Harwell, J. H. *J. Colloid Interface Sci.* **1988**, *123*, 186.
(32) Yuet, P. K.; Blankschtein, D. *Langmuir* **1996**, *12*, 3819.
(33) Guida, V. *Adv. Colloid Interface Sci.* **2010**, *161*, 77.
(34) Israelachvili, J. N.; Mitchell, D. J.; Ninham, B. W. *J. Chem. Soc., Faraday Trans.* **1976**, *72*, 1525.
(35) Mitchell, D. J.; Ninham, B. W. *J. Chem. Soc., Faraday Trans. 2* **1981**, *77*, 601.
(36) Hoffmann, H. *Adv. Mater.* **1994**, *6*, 116.
(37) Pupoa, E.; Padróna, A.; Santanaa, E.; Sotolongoa, J.; Quintanab, D.; Dueñasb, S.; Duarteb, C.; de la Rosac, M. C.; Hardyb, E. *J. Controlled Release* **2005**, *104*, 379.
(38) Bernard, A.l.; Guedeau-Boudeville, M. A.; Artzner, V. M.; Gulik-Krzywicki, T.; Meglio, J. M.; Jullien, L. *J. Colloid Interface Sci.* **2005**, *287*, 298.
(39) Lopez-Montero, I.; Rodrigez, N.; Cribier, S.; Pohl, A.; Velez, L.; Devaux, P. F. *J. Biol. Chem.* **2005**, *280*, 25811.
(40) Taneva, S. G.; Patty, P. J.; Frisken, B. J.; Cornell, R. B. *Biochemistry* **2005**, *44*, 9382.
(41) Tsogas, I.; Tsiourvas, D.; Nounesis, G.; Paleos, C. M. *Langmuir* **2005**, *21*, 5997.
(42) Namani, T.; Walde, P. *Langmuir* **2005**, *21*, 6210.
(43) Rossetti, F. F.; Bally, M.; Michel, R.; Textor, M.; Reviakine, I. *Langmuir* **2005**, *21*, 6443.
(44) Wang, H. Y.; Li, Y. M.; Xiao, Y.; Zhao, Y. F. *J. Colloid Interface Sci.* **2005**, *287*, 307.
(45) Fernadez, P.; Willenbacher, N.; Frechen, T.; Kuhnle, A. *Colloids Surf., A* **2005**, *262*, 204.
(46) Gradzielski, M. *J. Phys.: Condens. Matter* **2003**, *15*, 656.
(47) Khan, A.; Marques, E. F. *Curr. Opin. Colloid Interface Sci.* **2000**, *4*, 402.
(48) Šegota, S.; Težak, Đ. *Adv. Colloid Interface Sci.* **2006**, *121*, 51.
(49) Datta, A.; Pal, S. K.; Mandal, D.; Bhattacharyya, K. *J. Phys. Chem. B* **1998**, *102*, 6114.
(50) Dey, S.; Sasmal, D. K.; Das, D. K.; Bhattacharyya, K. *ChemPhysChem* **2008**, *9*, 2848.
(51) Dey, S.; Mandal, U.; Mojumdar, S. S.; Mandal, A. K.; Bhattacharyya, K. *J. Phys, Chem. B* **2010**, *114*, 15506.
(52) Vlachy, A; Arteaga, A. F.; Klaus, A.; Touraud, D.; Drechsler, M.; Kunz, W. *Colloids Surf., A* **2009**, *338*, 135.
(53) Mahiuddin, S.; Zech, O.; Raith, S.; Touraud, D.; Kunz, W. *Langmuir* **2009**, *25*, 12516.
(54) Yeh, S.-J.; Yang, Y.-M.; Chang, C.-H. *Langmuir* **2005**, *21*, 6179.
(55) Ho, C.; Stubbs, C. D. *Biochemistry* **1997**, *36*, 10630.
(56) Moreira, L. A.; Firoozabadi, A. *Langmuir* **2009**, *25*, 12101.
(57) Nakayama, H.; Shinoda, K.; Hutchinson, E. *J. Phys. Chem.* **1966**, *70*, 3502.
(58) Li, W.; Han, Y. C.; Zhang, J. L.; Wang, L. X.; Song, J. *Colloid J.* **2006**, *68*, 304.
(59) Rao, I. V.; Ruckenstein, E. *J. Colloid Interface Sci.* **1986**, *113*, 375.
(60) Vajda, S.; Jimenez, R.; Rosenthal, S. J.; Fidler, V.; Fleming, G. R.; Castner, E. W. J. *J. Chem. Soc., Faraday Trans.* **1995**, *91*, 867.
(61) Zhang, J.; Bright, F. V. *J. Phys. Chem.* **1991**, *95*, 7900.
(62) Riter, R. E.; Willard, D. M.; Levinger, N. E. *J. Phys. Chem. B* **1998**, *102*, 2705.
(63) Shirota, H.; Horie, K. *J. Phys. Chem. B* **1999**, *103*, 1437.
(64) Pant, D.; Levinger, N. E. *Langmuir* **2000**, *16*, 10123.
(65) Levinger, N. E. *Science* **2002**, *298*, 1722.
(66) Baumann, R.; Ferrante, C.; Deeg, F. W.; Brauchle, C. *J. Chem. Phys.* **2001**, *114*, 5781.
(67) Baumann, R.; Ferrante, C.; Kneuper, E.; Deeg, F. W.; Brauchle, C. *J. Phys. Chem. A* **2003**, *107*, 2422.
(68) Bhattacharyya, K.; Bagchi, B. *J. Phys. Chem. A* **2000**, *104*, 10603.
(69) Sen, S.; Sukul, D.; Dutta, P.; Bhattacharyya, K. *J. Phys. Chem. A* **2001**, *105*, 10635.
(70) Dutta, P.; Bhattacharyya, K. *J. Chem. Sci.* **2004**, *116*, 5.
(71) Hazra, P.; Chakrabarty, D.; Chakraborty, A.; Sarkar, N. *Chem. Phys. Lett.* **2004**, *388*, 150.

(72) Seth, D.; Chakraborty, A.; Setua, P.; Sarkar, N. *J. Chem. Phys.* **2007**, *126*, 224512.
(73) Balasubramanian, S.; Bagchi, B. *J. Phys. Chem. B* **2001**, *105*, 12529.
(74) Senapati, S.; Chandra, A. *J. Phys. Chem. B* **2001**, *105*, 5106.
(75) Feng, X.; Thompson, W. H. *J. Phys. Chem. C* **2010**, *114*, 4279.
(76) Nandi, N.; Bagchi, B. *J. Phys. Chem. B* **1997**, *101*, 10954.
(77) Nandi, N.; Bhattacharyya, K.; Bagchi, B. *Chem. Rev.* **2000**, *100*, 2013.
(78) Bhattacharyya, K. *Acc. Chem. Res.* **2003**, *36*, 95.
(79) Ghosh, S.; Mandal, U.; Adhikari, A.; Dey, S.; Bhattacharyya, K. *Int. Rev. Phys. Chem.* **2007**, *26*, 421.
(80) Rosenfeld, D. E.; Schmuttenmaer, C. A. *J. Phys. Chem. B* **2006**, *110*, 14304.
(81) Biswas, R.; Das, A. R.; Pradhan, T.; Touraud, D.; Kunz, W.; Mahiuddin, S. *J. Phys. Chem. B* **2008**, *112*, 6620.
(82) Sen, P.; Satoh, T.; Bhattacharyya, K.; Tominaga, K. *Chem. Phys. Lett.* **2005**, *411*, 339.
(83) Dutta, P.; Sen, P.; Mukherjee, S.; Bhattachayya, K. *Chem. Phys. Lett.* **2003**, *382*, 426.
(84) Bhattacharyya, K.; Bagchi, B. *J. Chem. Sci.* **2007**, *119*, 113.
(85) Arteaga, A. F. *Preparation, Characterization and Stability of O/W Emulsions and Microemulsions*. Ph.D. Thesis, University of Granada, Spain, 2006.
(86) Sovago, M.; Vartiainen, E.; Bonn, M. *J. Chem. Phys.* **2009**, *131*, 161107.
(87) Thewalt, J. L.; Wassall, S. R.; Gorrissen, H.; Cushley, R. J. *Biochim. Biophys. Acta* **1985**, *817*, 355.
(88) Ho, C.; Stubbs, C. D. *Biochemistry* **1997**, *36*, 10630.
(89) Dubey, N. *J. Chem. Eng. Data* **2010**, *55*, 1219.
(90) Reekmans, S.; Luo, H.; Van der Auweraer, M.; De Schryyer, F. C. *Langmuir* **1990**, *6*, 628.
(91) Horng, M. L.; Gardecki, J. A.; Papazyan, A.; Maroncelli, M. *J. Phys. Chem.* **1995**, *99*, 17311.
(92) Horng, M. L.; Gardecki, J. A.; Maroncelli, M. *J. Phys. Chem. A* **1997**, *101*, 1030.
(93) Renoncourt, A. *Study of Supra-aggregates in Catanionic Surfactant Systems*. Ph.D. thesis, University of Regensburg, Germany, 2005.
(94) Chakraborty, H.; Sarkar, M. *Langmuir* **2004**, *20*, 3551.
(95) Renoncourt, A.; Vlachy, N.; Bauduin, P.; Drechsler, M.; Touraud, D.; Verbavatz, J.-M.; Dubois, M.; Kunz, W.; Ninham, B. W. *Langmuir* **2007**, *23*, 2376.
(96) Ramsch, R.; Cassel, S.; Rico-Lattes, I. *Langmuir* **2009**, *25*, 6733.
(97) Harkins, W. D.; Mattoon, R. W.; Mittelmann, R. *J. Chem. Phys.* **1947**, *15*, 763.
(98) Caponetti, E.; Martino, D. C.; Floriano, M. A.; Triolo, R. *Langmuir* **1997**, *13*, 3277.
(99) Kalyanasundaram, K.; Thomas, J. K. *J. Am. Chem. Soc.* **1977**, *99*, 2039.
(100) Seimiarczuk, A.; Ware, W. R. *Chem. Phys. Lett.* **1990**, *167*, 263.
(101) Franks, N. P.; Abraham, M. H.; Lieb, W. R. *J. Pharm. Sci.* **1993**, *82*, 466.
(102) Triolo, A.; Russina, O.; Fazio, B.; Triolo, R.; Cola, E. D. *Chem. Phys. Lett.* **2008**, *457*, 362.
(103) Pradhan, T.; Ghoshal, P.; Biswas, R. *J. Chem. Sci.* **2008**, *120*, 275.
(104) Pradhan, T.; Ghoshal, P.; Biswas, R. *J. Phys. Chem. A* **2008**, *112*, 915.
(105) Nishikawa, K.; Hatashi, H.; Ijima, T. *J. Phys. Chem.* **1989**, *93*, 6559.
(106) Bowron, D. T.; Finney, J. L. *J. Phys. Chem. B* **2007**, *111*, 9838.
(107) Gazi, H. A. R.; Biswas, R. *J. Phys. Chem. A* **2011**, *115*, 2447.
(108) Gratzel, M.; Kalyanasundaram, K.; Thomas, J. K. *J. Am. Chem. Soc.* **1974**, *96*, 7869.
(109) Geiger, M.; Turro, N. J. *Photochem. Photobiol.* **1975**, *22*, 273.
(110) Biswas, R.; Lewis, J. E.; Maroncelli, M. *Chem. Phys. Lett.* **1999**, *310*, 485.
(111) Biswas, R.; Rohman, N.; Pradhan, T.; Buchner, R. *J. Phys. Chem. B* **2008**, *112*, 9379.
(112) Viscosities of the aqueous solutions of these catanionics in the presence of 0.05 *m* alcohol have been measured by using a suspended viscometer (Cannon-Ubelhode) at 298 K. During the *time of fall* measurements, the presence of a bubble over the meniscus prohibited the exact determination of the time required, and thus the error associated with each of the measurements is expected to be no less than ±10% of the reported values of solution viscosity.
(113) Fee, R. S.; Maroncelli, M. *Chem. Phys.* **1994**, *183*, 235.
(114) Jimenez, R.; Fleming, G. R.; Kumar, P. V.; Maroncelli, M. *Nature* **1994**, *369*, 471.
(115) Guchhait, B.; Gazi, H. A. R.; Kashyap, H. K.; Biswas, R. *J. Phys. Chem. B* **2010**, *114*, 5066.
(116) Gazi, H. A. R.; Guchhait, B.; Daschakraborty, S.; Biswas, R. *Chem. Phys. Lett.* **2011**, *501*, 358.
(117) Kashyap, H. K.; Biswas, R. *J. Phys. Chem. B* **2010**, *114*, 16811.
(118) Kashyap, H. K.; Biswas, R. *J. Phys. Chem. B* **2010**, *114*, 254.
(119) We do not understand why the decay of $S(t)$ should be single-exponential in the presence of pentanol while for other cases it is double-exponential. As a result, no specific significance has been attached to this observation.
(120) Shirota, H.; Tamoto, Y.; Segawa, H. *J. Phys. Chem. A* **2004**, *108*, 3244.
(121) Hara, K.; Kuwabara, H.; Kajimoto, O. *J. Phys. Chem. A* **2001**, *105*, 7174.
(122) Datta, A.; Mandal, D.; Pal, S. K.; Das, S.; Bhattacharyya, K. *J. Mol. Liq.* **1998**, *77*, 121.
(123) Sarkar, N.; Datta, A.; Das, S.; Bhattacharyya, K. *J. Phys. Chem.* **1996**, *100*, 15483.
(124) Tamoto, Y.; Segawa, H.; Shirota, H. *Langmuir* **2005**, *21*, 3757.
(125) Arzhantsev, S.; Jin, H.; Baker, G. A.; Maroncelli, M. *J. Phys. Chem. B* **2007**, *111*, 4978.
(126) Jin, H.; Baker, G. A.; Arzhantsev, S.; Maroncelli, M. *J. Phys. Chem. B* **2007**, *111*, 7291.
(127) Ito, N.; Arzhantsev, S.; Heitz, M.; Maroncelli, M. *J. Phys. Chem. B* **2004**, *108*, 5771.
(128) Kalita, G.; Rohman, N.; Mahiuddin, S. *J. Chem. Eng. Data* **1998**, *43*, 148.
(129) Jin, H.; O'Hare, B.; Dong, J.; Arzhantsev, S.; Baker, G. A.; Wishart, J. F.; Benesi, A. J.; Maroncelli, M. *J. Phys. Chem. B* **2008**, *112*, 81.
(130) Das, A.; Biswas, R.; Chakrabarti, J. Solute Rotation in Polar Liquids: Microscopic Basis for the SED Model. *J. Phys. Chem. B* **2011** submitted for publication.